Optimized Charging in Large-Scale Deployed WSNs with Mobile Charger

Zhenquan Qin[1], Bingxian Lu[1], Ming Zhu[1], Liang Sun[1], and Lei Shu[2]
[1] School of Software, Dalian University of Technology
Dalian, Liaoning 116000 - CN
[e-mail: zhuming@dlut.edu.cn]
[2] Guangdong Petrochemical Equipment Fault Diagnosis Key Laboratory,
Guangdong University of Petrochemical Technology,
Maoming, Guangdong 525000 - CN
[e-mail: lei.shu@lab.gdupt.edu.cn]
*Corresponding author: Ming Zhu

Received January 1, 2016; revised June 3, 2016; revised August 13, 2016; accepted November 17, 2016; published December 31, 2016

Abstract

Restricted by finite battery energy, traditional wireless sensor networks (WSNs) can only maintain for a limited period of time, resulting in serious performance bottleneck in long-term deployment of WSN. Fortunately, the advancement in the wireless energy transfer technology provides a potential to free WSNs from limited energy supply and remain perpetual operational. A mobile charger called wireless charging vehicle (WCV) is employed to periodically charge each sensor node and keep its energy level above the minimum threshold. Aiming at maximizing the ratio of the WCV's vocation time over the cycle time as well as guaranteeing the perpetual operation of networks, we propose a feasible and optimal solution to this issue within the context of a real-time large-scale deployed WSN. First, we develop two different types of charging cycles: initialization cycles and renewable cycles and give relevant algorithms to construct these two cycles for each sensor node. We then formulate the optimization problem into an optimal construction algorithm and prove its correctness through theoretical analysis. Finally, we conduct extensive simulations to demonstrate the effectiveness of our proposed algorithms.

Keywords: Lifetime, Optimization, Wireless Power Transfer, Wireless Sensor Networks

A preliminary version of this paper appeared in IEEE GLOBECOM 2015, December 6-10, San Diego, USA. This work is supported by Natural Science Foundation of China under Grants No. 61070181, No. 61272524 and No. 61202442 and the Fundamental Research Funds for the Central Universities. This work of Lei Shu is supported by 2013 Special Fund of Guangdong Higher School Talent Recruitment, Educational Commission of Guangdong Province, China Project No. 2013KJCX0131, Guangdong High-Tech Development Fund No. 2013B010401035, National Natural Science Foundation of China (Grant NO. 61401107). This work is also supported by the Fundamental Research Funds for the Central Universities under Grants No. DUT14ZD218 and No. DUT14QY29.

http://dx.doi.org/10.3837/tiis.2016.12.010 **ISSN : 1976-7277**

1. Introduction

For traditional wireless sensor network (WSN) applications, sensor nodes are usually powered by batteries with limited energy capacity. This finite energy supply brings urgent performance bottleneck to the long-term maintenance in wide-range WSN deployment. Therefore, many efforts, including energy conservation [1,2], energy harvesting [3,4], and sensor reclamation [5], have been devoted to prolonging the lifetime of WSNs. Despite these intensive research works, network lifetime remains a big challenge in practical applications. Although energy scavenging techniques have been greatly developed to extract energy from renewable energy sources like solar, wind, vibration etc., their practical availability remains limited due to the environmental constraints. In recent years, Kurs et al. [6] have exploited the magnetic resonance techniques to transfer energy from one power source to a receiver without any plugs or wires, which opened up a new dimension for extending the lifetime of sensor networks. Specifically, the reported experiment [7] also demonstrated that it is possible to transfer 60 watts of power over a distance of up to two to three feet with a high efficiency of 75%.

Inspired by this technology breakthrough, many applications utilizing wireless energy transfer in WSNs emerged like mobile data gathering [8]. Particularly, research efforts begin to seek reliable mechanisms and strategies to address recharging scheduling problem in wireless sensor networks. Among these literatures, a mobile charger is employed to traverse around the WSN field and transfer energy to sensor nodes wirelessly. Yi Shi et al. [9,10] proposed an optimal routing and charging policy with the objective of maximizing the staying time at service station of the mobile charger, which is too static to be applied in a practical WSN. Similarly, Z. Li et al. [11] studied a practical joint routing and charging scheme aiming to employ energy-balanced routing and energy-minimum routing in a balanced way. In [12,13], a new charging paradigm involved multiple mobile chargers was studied to solve collaborative charging scheduling problem, which is incomplete and complicated to realize. In addition, authors in [14,15] investigated on-line charging scheduling algorithms according to the spatial and temporal properties of sensor nodes. Either a probabilistic mechanism or frequent information exchanges among sensor nodes are involved in these researches.

In this paper, we focus on addressing recharging scheduling problem in practical deployed large-scale wireless networks where it's hard to pre-configure each sensor node to satisfy certain routing requirements. Our algorithms can be applied to environment monitoring wireless sensor networks where node periodically sends data to the sink node and has a stable energy consumption rate. When the energy consumption rate is varied, our model needs to be modified but still has great significance. Our main contributions are the followings:

- We formulate the wireless energy transfer scheduling problem into an optimization problem aiming at maximizing the ratio of the mobile charger's vacation time over the charging cycle time as in [9]. A mobile charger called WCV is employed to periodically charge each sensor node to keep the whole WSN perpetual operation. Our strategy generates little extra message exchange overhead only at the beginning of the system.
- We develop two different charging cycles: one is initialization cycles and the other is renewable cycles during a sensor node's life time. We offer two corresponding construction algorithms and prove their correctness through theoretical analysis. Several interesting properties and lemmas are discovered and proved. We also consider

various scenarios when performing the algorithms and give corresponding solutions at a small price. Our algorithms are easy to be implemented in a practical deployed wireless sensor network.

- Based on theoretical analysis, we present simulation results to evaluate the proposed algorithms. By showing numerical results, we demonstrate the effectiveness of our algorithms which achieve expected performance. In addition, we discuss extending case when WSNs become larger and more complicated.

The remainder of this paper is organized as follows. We describe the mathematical model and specify the optimization objective in section 2. In section 3, we discuss the construction of renewable energy cycles and give the theoretical proofs. In section 4, we explore the construction of initialization cycles. Simulation results are presented in section 5. Section 6 concludes the paper.

2. Mathematical Modeling

2.1 Background Description

We consider the scenario of a set of sensor nodes N, indexed by $1,2,..,n \in N$, randomly scattered over a two-dimensional plane. Each sensor node is fully charged initially with a maximum battery energy capacity of E_{max}. To keep each sensor node operational, it must have an energy level above E_{min}. There is a fixed base station within the WSN, which is the sink node for all data generated by sensor nodes. Multi-hop routing is used for forwarding data to the sink node. Let P_i denote the energy consumption rate for each sensor node, we will later discuss data routing and energy consumption of sensor nodes.

A mobile charger called wireless charging vehicle (WCV) is employed to charge each sensor node only once along a path designed beforehand. The time spent for charging a single sensor node is denoted as t_i. The total time for charging of WCV T_c is

$$T_c = \sum_{i=1}^{n} t_i. \tag{1}$$

In this paper, we consider the case where only one mobile charger is available in the WSN and by partitioning, our approach can be extended to a more complicated scenario where a large-scale WSN with thousands of nodes is deployed and several mobile chargers are required, which will be discussed in the last subsection. In addition, the WCV employed in our paper is assumed to have enough energy or say, to have been refueled so that it is capable of implementing charging tasks and traveling. The sink node notifies WCV of the WSN's global knowledge and the charging schedule via a long range radio. We assume that WCV departs from the service station and returns back to it when WCV accomplishes the scheduling tasks. When WCV is not assigned charging tasks, it stays at the service station to receive maintenance service (taking a vocation or replenishing energy quantity), and this period of service time is denoted as T_{vac}. We assume WCV moves along the straight line between sensor nodes, and it travels inside the WSN at a speed of Vm/s which can be adjusted like a real mobile vehicle. In renewable cycles (defined later), WCV travels at a constant speed of V. Let $p(N_0, N_1, N_2, \ldots, N_n)$ denote the designed traveling path for WCV, in which $N_0, N_1, N_2, \ldots, N_n$ are the index numbers of sensor nodes. Let $N_0 = 0$ denote the index number for service station. We also let $d_{i,j}$ denote the distance from node i to node j and the time for WCV to move from node i to node j is denoted as $t_{i,j} = \frac{d_{i,j}}{V}$. Then we have the total time for traveling the physical path $T_p = \sum_{i=0,j=i+1}^{i=n} t_{N_i,N_j}$, when i=n, j=0. T is denoted as the overall time spent during a charging cycle, it holds:

$$T = T_{vac} + T_c + T_p. \tag{2}$$

Let U_i denote the power reception rate at sensor node i and $U_i = \mu(D_i) \cdot U_{Full}$, where D_i is the distance from the node i to WCV and U_{Full} is the full output power from the WCV for a single sensor node and $\mu(D_i)$ is the efficiency of wireless power transfer. Note that $\mu(D_i)$ is a decreasing function with respect to D_i and $0 \le \mu(D_i) \le 1$. When $D_i = 0$, U_i achieves the maximum value U_{Full}. According the curve fitting result in [10], we have the efficiency of wireless power transfer:

$$\mu(D_i) = -0.0958 \times D_i^2 - 0.0377 D_i + 1.0. \tag{3}$$

We also assume that when WCV is charging only one single node at one time, energy level of other nodes nearby will not get affected (because they will turn off the energy reception module of the battery if they are not scheduled to be charged).

In our optimization problem, our ultimate goal is to keep the whole WSN operational forever with an efficient charging schedule. To satisfy the elementary requirement, i.e. each sensor node must have an energy level above E_{min} at any time. Here, we carry on the definition of renewable energy cycle in [9] that the energy level of a sensor node i should meet the following two requirements: i) it starts and ends with the same energy level over a charging cycle. ii) it never falls below E_{min}. Let E_i denote the energy level at the beginning of a renewable energy cycle, A_i denote the time span from the beginning of a cycle to the time point when WCV arrives at node i. Note that $U_i \cdot t_i \ge T \cdot P_i$ must be satisfied in each renewable cycles, the former shows the amount of energy being charged to node i during the time period of t_i, while the latter shows the amount of energy consumed during the cycle. It can be easily proved by showing that if $\boldsymbol{U_i \cdot t_i < T \cdot P_i}$, then the energy of node i will fall below E_{min} eventually at some time t. To meet the definition of "renewable energy cycle" above, we have the following constraints:

$$E_i - A_i \cdot P_i \ge E_{min}. \tag{4}$$

$$U_i \cdot t_i = T \cdot P_i. \tag{5}$$

Equation (5) obviously ensures the first requirement in the definition. Let Ec_i denote the energy level of node i at the time when WCV arrives, then $Ec_i = E_i - A_i \cdot P_i$ is the lowest energy level during a charging cycle, if (4) holds, the energy level of a sensor node at any time point will be above E_{min}, which ensures the second requirement in the definition.

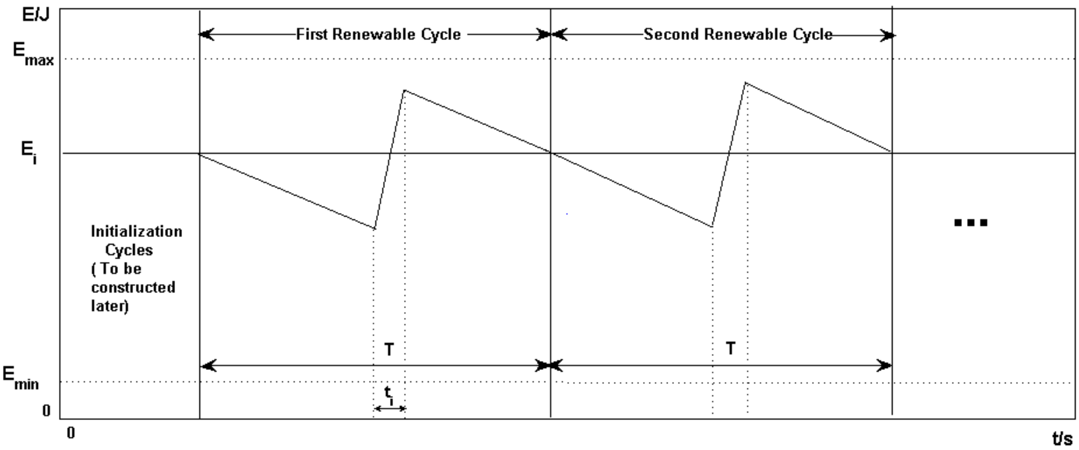

Fig. 1. An example of the energy level of node i during the first two renewable cycles.

The energy-time diagram of node i is shown as **Fig. 1** Naturally, each sensor node has an energy level of E_{max} initially before being put into use. So, how to initialize the energy level E_i for each node i without against the purpose of employing the approach in a large-scale WSN is our objective. We divide charging cycles into two types: initialization cycles and renewable cycles, among which the latter one conforms to the definition of “renewable energy cycle”. We will give the construction algorithms for the two charging cycles in later sections.

2.2 Data Flow Routing and Energy Consumption

Let f_{ij} and f_{iB} denote the flow rates from sensor node i to sensor node j and the base station B, respectively. Each sensor node i generates sensing data with a rate C_i (in kb/s), $i \in N$. We have the flow rate constraint at each node i as follows to guarantee that the total amount of data rates flowing into a node i is equal to that flowing out of it.

$$\sum_{k \in N}^{k \neq i} f_{ki} + C_i = \sum_{j \in N}^{j \neq i} f_{ij} + f_{iB} \ \ (i \in N). \tag{6}$$

Our energy consumption model at each sensor node is partly based on [16]. A wireless sensor node can be considered as composed by several modules including sensor module, processor module, communication module and energy supply module, among which the sensor module, processor module and communication module consume energy during the working state of a sensor node [17]. With the advances in integrated circuit technology, the power consumption of the processor and sensor modules is low. Wireless communication module could stay in data transmission, data reception, idle and sleep state. A sensor node monitors signals from other nodes but does not send or receive data in idle state. And in sleep state, a sensor node does not work. **Fig. 2** shows the energy consumption of each module of a common wireless sensor node. Let θ_{ij} denote the rate of energy consumption for transmitting one bit data from node i to node j, as discussed:

$$\boldsymbol{\theta_{ij} = \varepsilon_1 + \varepsilon_2 d_{ij}^{\alpha}}.$$

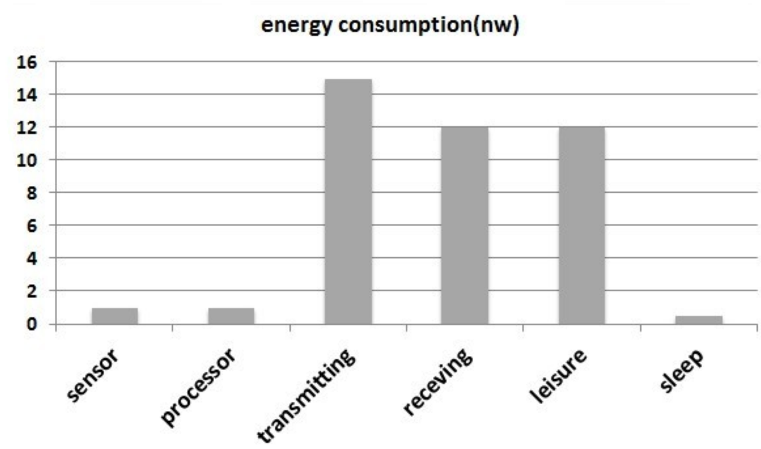

Fig. 2. Energy consumption of each module in a common wireless sensor node.

Where ε_1 is a distance-independent constant term, ε_2 is a coefficient of the distance-dependent term, d_{ij} is the distance between nodes i and j and α is the path loss index. Thus, to transmit a flow rate of f_{ij} from node i to node j, the transmission power is $\theta_{ij} \times f_{ij}$. Let θ_{iB} be the rate of energy consumption for transmitting one bit data rate from node i to the base station B. Then the aggregate energy consumption rate for transmission at node i, which is denoted as P_i^{tx}, is

$$P_i^{tx} = \sum_{j \in N}^{j \neq i} \theta_{ij} f_{ij} + \theta_{iB} f_{iB}.$$

Similarly, the energy consumption rate P_i^{rx} for data reception at node i has the following equation:

$$P_i^{rx} = \sigma \sum_{k \in N}^{k \neq i} f_{ki}.$$

Where σ is the rate of energy consumption for receiving one bit data.

From **Fig. 2**, we know that the energy consumed during free time is almost equal to the energy consumed by data reception, we thus assume they are equal to simplify the energy consumption model. We let P_i^{fx} denote the energy consumed during free time of a wireless sensor node. Then, we have:

$$P_i^{fx} = \sigma \sum_{k \in N}^{k \neq i} f_{ki}.$$

Based on the energy consumption model discussed above, the total energy consumption rate at sensor node $i \in N$, P_i, including energy consumption for transmission, reception and monitoring in idle state, is modeled as

$$P_i = 2\sigma \sum_{k\in N}^{k\neq i} d_{ki} + \sum_{j\in N}^{j\neq i} \theta_{ij}\, d_{ij} + \theta_{iB} d_{iB}. \tag{7}$$

Given a deployed WSN in which each sensor node is uniformly randomly scattered over an area and given relevant constant terms, we could calculate the energy consumption rate P_i for each node i. Thus, P_i is invariant during our analysis. Previous work, such as [9, 10], deals only with unconfigured WSN in which flow rates and routing solution are included in the optimization variables. Suppose a set of solution is given and the WSN is composed of thousands of sensor nodes, to configure the flow rate and routing table for each sensor node according to the optimization result is really a tough job to complete. Therefore, it's impractical to apply these optimal solutions to a large-scale WSN. We give a solution to the same optimization objective but within a large-scale WSN context, i.e. we do the optimization for a deployed WSN instead of a devoid one.

2.3 Optimization Objective

In order to make WCV accomplish its charging tasks efficiently, we target at maximizing the ratio of vacation time T_{vac} over the total cycle time T, or equivalently, to minimize the percentage of time when WCV is out for charging work. We assume the distance between WCV and sensor node is 0 during the period of charging, i.e. the power reception rate of each sensor node i is U_{Full} during renewable cycles. With the definition of "renewable energy cycle" above, we can see that if the energy consumption rate P_i is determined for every sensor node, the total charging time T_c is an overall cycle time T dependent term as follows:

$$T_c = \sum_{i=1}^{i=n} t_i = \frac{T}{U_{Full}} \cdot \sum_{i=0}^{n} P_i. \tag{8}$$

And we denote $\sum_{i=0}^{n} P_i$ as P_s. Here we rewrite (2):

$$T = T_{vac} + T_c + T_p.$$

Divide both sides by T, we get:

$$\frac{T_{vac}}{T} = 1 - \frac{T_c}{T} - \frac{T_p}{T} = 1 - \frac{P_s}{U_{Full}} - \frac{T_p}{T}. \tag{9}$$

As $\frac{P_s}{U_{Full}}$ is a constant term once a WSN is deployed, we see from equation (9) that to maximize our objective $\frac{T_{max}}{T}$, we just need to minimize the term $\frac{T_p}{T}$, which is a nonlinear term. But in this nonlinear term, T_p is the time for traveling path, so we naturally think of the Traveling Salesman Path (Tsp path). No matter what the total cycle time T is, a Tsp path will apparently take the shortest time for WCV traveling. So, we just select the Tsp path and solve a maximum feasible T under this condition. In this way we can get the optimal solution to $\frac{T_{max}}{T}$.

3. Construction of Renewable Cycle

From the Energy-Time diagram of a node i (see **Fig. 1**), there are only two possible slopes for any renewable cycle: i) a slope of $-P_i$ when WCV is not charging the node. ii) a slope of $(U_{Full} - P_i)$ when WCV is charging the node. Small figures (a), (b), (c), (d) in **Fig. 3** are used to help understand the construction process.

3.1 Feasible T

In this part, we will solve the problem when T is suitable for each node. In **Fig. 3(a)**, first we draw a line l_1 with a slope of $-P_i$ and it intersects $E = E_{min}$ at A, which represents the lowest point at which node i can be saved by WCV, or the node will "die" when its energy level is below E_{min}. With the following equation set, we can solve point $A(\frac{E_i - E_{min}}{P_i}, E_{min})$.

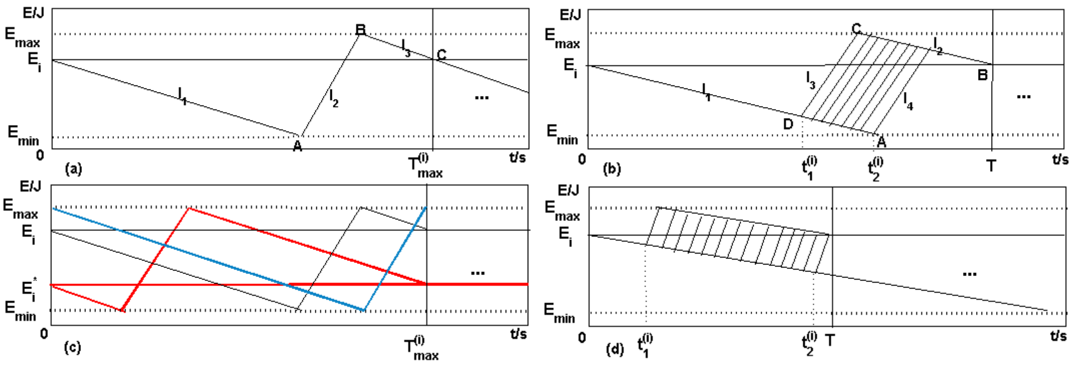

Fig. 3. The diagram of energy-time of node i.

$$\begin{cases} l_1: E = -P_i \cdot t + E_i, \\ E = E_{min}. \end{cases}$$

Then, through point A we draw another line l_2 which has a slope of $(U_{Full} - P_i)$ and it intersects $E = E_{max}$ at point B, which represents the highest point at which node i could receive energy from WCV, or the energy level will exceed the E_{max} . We can solve $B(\frac{E_{max}-E_{min}}{U_{Full}-P_i} + \frac{E_i - E_{min}}{P_i}, E_{max})$ from the following equation set and we write B as $B(B_t, E_{max})$:

$$\begin{cases} l_2: E - E_{min} = (U_{Full} - P_i) \cdot (t - \dfrac{E_i - E_{min}}{P_i}), \\ E = E_{max}. \end{cases}$$

Next, we draw the third line l_3 through B with a slope of $-P_i$ and it intersects the line $E = E_i$ at $C(\frac{E_{max}-E_{min}}{P_i} + \frac{E_{max}-E_{min}}{U_{Full}-P_i}, E_i)$.

$$\begin{cases} l_3: E - E_{max} = -P_i \cdot (t - B_t), \\ E = E_i. \end{cases}$$

The horizontal axis of C is the max T we solve for node i, which is denoted as $T_{max}^{(i)}$,

$$T_{max}^{(i)} = \frac{E_{max} - E_{min}}{P_i} + \frac{E_{max} - E_{min}}{U_{Full} - P_i}. \tag{10}$$

Which is the extreme cycle time for node i, i.e. the total cycle time T can not exceed this $T_{max}^{(i)}$, otherwise, to meet the definition of renewable energy cycle, i.e. equation (5), the WCV has to charge it over E_{max} but E_{max} is the full energy capacity of a sensor node. It can be easily seen by moving $t = T_{max}^{(i)}$ to right.

Property 1. $T_{max}^{(i)}$ is independent on E_i and only determined by the node i's energy consumption rate P_i.

We can easily find this property in equation (10). **Fig. 3(c)** depicts this interesting property: a node i is given an initial energy level of E_i(black lines) and E_i^*(red lines) respectively, but we can see they achieve the same $T_{max}^{(i)}$. Take an extreme case into consideration, says $E_i = E_{max}$, which is also shown in **Fig. 3(c)** in blue lines, it also achieves the same $T_{max}^{(i)}$ and in this case, the total charging cycle is end as soon as node i is charged to E_{max}.

Based on the discussion above, we can solve $T_{max}^{(i)}$ for every node i, to have all the nodes satisfying the energy constraints, i.e. the definition of renewable energy cycle, a feasible T must be less than or equal to $min\{T_{max}^{(i)}\}$ as follows, and $min\{T_{max}^{(i)}\}$ is denoted as T^*:

$$T \le min\{T_{max}^{(i)}\}. \tag{11}$$

Note that U_{Full} is usually much greater than P_i, then $\frac{E_{max}-E_{min}}{U_{Full}-P_i} \approx \frac{E_{max}-E_{min}}{U_{Full}}$, so $T_{max}^{(i)}$ is mainly determined by P_i, and T^* is very likely to be determined by node i whichhas a greater P_i.

3.2 Chargeable range

Suppose $T \in (0, min\{T_{max}^{(i)}\})$ is the overall time of a charging cycle, then we can find a time range for each node i during which the WCV can arrive at it and charge it at any time point and we call this time range of node i "chargeable range", denoted as $\tau_i = [t_1^{(i)}, t_2^{(i)}]$, which is shown in **Fig. 3(b)**: we first draw two lines l_1, l_2 with a slope of $-P_i$ through $(0, E_i)$ and point B respectively. Through the two intersections A and C we can draw another two lines $l_3, l_4$with a slope of $(U_{Full} - P_i)$. l_3 intersects l_1 at D. The horizontal axes of D and A, $t_1^{(i)}, t_2^{(i)}$, are the left and right boundary of the chargeable range τ_i. Then let's solve this τ_i. First we can solve $A(\frac{E_i-E_{min}}{P_i}, E_{min})$ with the method in last part and also we know $B(T, E_i)$. Then we can express l_2 and solve $C(T + \frac{E_i-E_{max}}{P_i}, E_{max})$:

$$\begin{cases} l_2: E - E_i = -P_i \cdot (t - T), \\ E = E_{max}. \end{cases}$$

Then, we get the expression of l_3 and solve $D(T - (\frac{E_{max}-E_i}{P_i} + \frac{T \cdot P_i}{U_{Full}}), E_{max} + P_i(\frac{T \cdot P_i}{U_{Full}} - T))$:

$$\begin{cases} l_3: E - E_{max} = (U_{Full} - P_i)(t - T - \frac{E_i - E_{max}}{P_i}), \\ l_1: E = -P_i \cdot t + E_i. \end{cases}$$

We rewrite $t_1^{(i)}$ and $t_2^{(i)}$ here:

$$t_1^{(i)} = T - (\frac{E_{max} - E_i}{P_i} + \frac{T \cdot P_i}{U_{Full}}). \tag{12}$$

$$t_2^{(i)} = \frac{E_i - E_{min}}{P_i}. \tag{13}$$

we can get the length of the chargeable range τ_i, i.e. $t_2^{(i)} - t_1^{(i)}$, denoted as Δ_i:

$$\Delta_i = \frac{E_{max} - E_{min}}{P_i} + \frac{T \cdot P_i}{U_{Full}} - T. \tag{14}$$

If the WCV's arrival time at node i is not in τ_i, then it will breach the requirements of renewable energy cycle, e.g. if the WCV arrives at the left side of τ_i to charge node i in advance, the energy level of node i at the end of the renewable cycle will fall below E_i and if WCV arrives at the right side of τ_i to charge node i, the energy level of node i has already fallen below E_{min} when WCV arrives.

Property 1. Given T, $t_1^{(i)}, t_2^{(i)}$, which are all dependent on E_i and P_i, Δ_i is a term independent from E_i, only determined by P_i.

We find this property from equations (12)-(14). An intuitive explanation we can get from this property is that for a fixed P_i, E_i controls the position of the chargeable range τ_i on the horizontal axis, e.g. a higher E_i moves the whole chargeable range to the left. Note that the Δ_i is a check mark function of $P_i (P_i > 0)$, and the lowest point achieves at $P_i = \sqrt{\frac{\frac{E_{max} - E_{min}}{T}}{U_{Full}}}$, denoted as P_σ. If T is quiet small for node i and $|P_i - P_\sigma|$ is quiet large, Δ_i may cover most of T or even greater than T(in this case $t_1 \leq 0, t_2 \geq T$), as shown in **Fig. 3(d)**.

3.3 Construction Algorithm

From section 2.3, we know that to obtain the maximum objective value $\frac{T_{vac}}{T}$, WCV needs to follow Tsp path to travel through each node, in the meanwhile, T is required to reach its maximum value. From equation (11), we get $T_{max} = T^* = min\{T_{max}^{(i)}\}$. Now we determine the energy level of a sensor node i at the beginning of the renewable energy cycle. Note that $t_2^{(i)}$ is the right bound of τ_i, at which WCV can arrive at node i and charge it. To develop a feasible charging sequence in Tsp order, we solve corresponding E_i by taking $t_2^{(i)}$ as the WCV arrival time as follows. For the sake of simplicity, U in this section means U_{Full}.

Algorithm 1. Reindex the sensor nodes according to the WCV traveling order (Tsp order) as $(0,1,2,\cdots,n)$, where 0 represents the service station. Given charging cycle length $T = T^*$ and WCV arrival time points at each nodes, $t_2^i, i = 1,2,\cdots,n$.We have the following equations:

$$t_2^n + t_n + t_{n,0} = T.$$
$$t_2^i + t_i + t_{i,i+1} = t_2^{i+1},\ i = 1,2,\cdots,n-1.$$

where $t_2^i = \frac{E_i - E_{min}}{P_i}$,$t_i = \frac{P_i T}{U}$, $i = 1,2,\cdots,n-1$, $t_{i,i+1}$ is the time for WCV to travel from node i to node $i+1$, P_i can be solved with equation (7), U, E_{max}, E_{min} are constants. Thus, E_i can be solved in the reverseorder of Tsp, i.e. $E_n, E_{n-1}, \cdots, E_1$.

Rewriting these equations gives

$$E_i = \begin{cases} \left(T - \frac{T}{U}\sum_{k=i}^{n} P_k - \sum_{k=i}^{n-1} t_{k,k+1} - t_{n,0}\right) P_i + E_{min}, if\ i = 1,2,\cdots,n-1. \\ (T - \frac{P_n T}{U} - t_{n,0}) P_n + E_{min},\quad if\ i = n. \end{cases}$$

Lemma 1. For given $\{P_i\}_{i=1,2,\ldots,n}$, E_{max}, E_{min}, U, T, $t_{n,0}$, $\{t_{k,k+1}\}_{k=1,2,\ldots,n-1}$, $E_i > E_{min}$ for all $i = 1,2,\ldots,n$.

Since $T = T_{vac} + T_c + T_p = T_{vac} + \frac{T}{U}\sum_{k=1}^{n} P_k + \sum_{k=0}^{n-1} t_{k,k+1} + t_{n,0}$, then

$$T - \frac{T}{U}\sum_{k=i}^{n} P_k - \sum_{k=i}^{n-1} t_{k,k+1} - t_{n,0} = \begin{cases} T_{vac} + \frac{T}{U}\sum_{k=1}^{i-1} P_k + \sum_{k=0}^{i-1} t_{k,k+1} > 0, i = 1,2,\ldots,n-1. \\ T_{vac} + t_{0,1} > 0, i = 1. \end{cases}$$

$$T - \frac{P_n T}{U} - t_{n,0} = T_{vac} + \frac{T}{U}\sum_{k=1}^{n-1} P_k + \sum_{k=0}^{n-1} t_{k,k+1} > 0.$$

Note that $P_i > 0, i = 1,2,\ldots,n$, thus

$$(T - \frac{T}{U}\sum_{k=i}^{n} P_k - \sum_{k=i}^{n-1} t_{k,k+1} - t_{n,0}) P_i > 0.$$

$$(T - \frac{P_n T}{U} - t_{n,0}) P_n > 0.$$

It follows that $E_i > E_{min}$ for all $i = 1,2,\ldots,n$

Lemma 2. For $i = 1,2,\ldots,n-1$, $E_i \le E_{max}$ if

$$(I)\, \frac{T}{U}\sum_{k=i}^{n} P_k + \sum_{k=i}^{n-1} t_{k,k+1} + t_{n,0} \ge \frac{UP_i - UP_{max} + P_{max}^2}{P_{max}(U - P_{max})P_i}(E_{max} - E_{min}).$$

For $i = n$, $E_i \le E_{max}$ if

$$(II)\ \frac{TP_n}{U} + t_{n,0} \ge \frac{UP_n - UP_{max} + P_{max}^2}{P_{max}(U - P_{max})P_n}(E_{max} - E_{min}).$$

From the argument above, we have

$$T = min\{T_{max}^{(i)}\} = min\{\frac{E_{max} - E_{min}}{P_i} + \frac{E_{max} - E_{min}}{U - P_i}\}.$$

Now to consider the monotonic property of function $\frac{E_{max}-E_{min}}{P_i} + \frac{E_{max}-E_{min}}{U-P_i}$ with respect to P_i by differentiating the function with respect to P_i. Since

$$(\frac{E_{max} - E_{min}}{P_i} + \frac{E_{max} - E_{min}}{U - P_i})' = (E_{max} - E_{min})[\frac{1}{(U - P_i)^2} - \frac{1}{P_i^2}] < 0.$$

if and only if $P_i < \frac{U}{2}$, then
$\frac{E_{max}-E_{min}}{P_i} + \frac{E_{max}-E_{min}}{U-P_i}$ is monotonically decreasing with respect to P_i when $P_i < \frac{U}{2}$ ($P_i << \frac{U}{2}$ in practice), and hence

$$T = min\{\frac{E_{max} - E_{min}}{P_i} + \frac{E_{max} - E_{min}}{U - P_i}\} = \frac{E_{max} - E_{min}}{P_{max}} + \frac{E_{max} - E_{min}}{U - P_{max}}.$$

For $i = 1,2,\dots,n-1$,

$$\begin{aligned}
E_i &= (T - \frac{T}{U}\sum_{k=i}^{n} P_k - \sum_{k=i}^{n-1} t_{k,k+1} - t_{n,0})P_i + E_{min} \\
&= (\frac{P_i}{P_{max}} + \frac{P_i}{U - P_{max}})(E_{max} - E_{min}) + E_{min} - (\frac{T}{U}\sum_{k=i}^{n} P_k + \sum_{k=i}^{n-1} t_{k,k+1} + t_{n,0})P_i \\
&\le \frac{P_i U}{P_{max}(U - P_{max})}(E_{max} - E_{min}) + E_{min} - \frac{UP_i - UP_{max} + P_{max}^2}{P_{max}(U - P_{max})P_i}(E_{max} - E_{min})P_i \\
&\le \frac{P_{max}(U - P_{max})}{P_{max}(U - P_{max})}(E_{max} - E_{min}) + E_{min} = E_{max}.
\end{aligned}$$

Also,

$$\begin{aligned}
E_n &= (T - \frac{P_n T}{U} - t_{n,0})P_n + E_{min} \\
&= (\frac{P_n}{P_{max}} + \frac{P_n}{U - P_{max}})(E_{max} - E_{min}) + E_{min} - (\frac{P_n T}{U} + t_{n,0})P_n \\
&\le \frac{P_{max}(U - P_{max})}{P_{max}(U - P_{max})}(E_{max} - E_{min}) + E_{min} = E_{max}.
\end{aligned}$$

Therefore, the sufficiency of condition(I) and condition(II) have been proved.

Remark 1. For any P_i, $i = 1,2,\dots,n$, such that

$$0 < P_i \le P_{max} - \frac{P_{max}^2}{U},$$

we have

$$\frac{UP_i - UP_{max} + P_{max}^2}{P_{max}(U - P_{max})P_i}(E_{max} - E_{min})$$
$$\leq \frac{UP_{max} - P_{max}^2 - UP_{max} + P_{max}^2}{P_{max}(U - P_{max})P_i}(E_{max} - E_{min}) = 0.$$

Hence, if $i \neq n$, condition (I) is satisfied naturally; if $i = n$, condition (II) is satisfied naturally.

From Remark 1, we know that when P_i doesn't satisfy $P_i \in (0, P_{max} - \frac{P_{max}^2}{U})$, node i may not satisfy condition (I) or condition (II) in Lemma 2. The following lemma shows that giving some extra attention to a node could have all nodes satisfy $E_i \leq E_{max}$.

Lemma 3. For an arbitrary sequence of $\{P_i\}_{i=1,2,\ldots,n}$, and an arbitrary integer m between 1 and n, let

$$P_i^{(m)} = \begin{cases} P_i, & if\ i \neq m, \\ \frac{U - \sqrt{U^2 - 4UP_{max}}}{2}, & if\ i = m. \end{cases}$$

where $P_{max} = max_{i=1,2,\ldots,n}\{P_i\}$, then for the new sequence of $\{P_i^{(m)}\}_{i=1,2,\ldots,n}$,

$$E_i^{(m)} \leq E_{max},\ for\ all\ i \neq m.$$

where $E_i^{(m)}$ is the energy level of a sensor node i at the beginning of the renewable energy cycle given $\{P_i^{(m)}\}_{i=1,2,\ldots,n}$.

Since

$$P_m^{(m)} - \frac{(P_m^{(m)})^2}{U} = \frac{U - \sqrt{U^2 - 4UP_{max}}}{2} - \frac{(\sqrt{U^2 - 4UP_{max}})^2}{4U} = P_{max},$$

and $\frac{(P_m^{(m)})^2}{U} > 0$, then $P_m^{(m)} > P_{max}$.

Hence,

$$max_{i=1,2,\ldots,n}\{P_i^{(m)}\} = P_m^{(m)} =: P_{max}^{(m)}.$$

Note that for $i \neq m$,

$$P_i^{(m)} = P_i \leq P_{max} = P_m^{(m)} - \frac{(P_m^{(m)})^2}{U}.$$

So, based on the remark 1, condition (I) is satisfied when $i \neq n$ and condition (II) is satisfied when $i = n$.

Therefore,

$$E_i^{(m)} \leq E_{max},\ for\ all\ i \neq m.$$

Remark 2. For $m \neq n$, the sufficient condition for $E_m^{(m)} \leq E_{max}$ is

$$\frac{T^{(m)}}{U}\sum_{k=m}^{n} P_k^{(m)} + \sum_{k=m}^{n-1} t_{k,k+1} + t_{n,0} \geq \frac{1}{U - P_m^{(m)}}(E_{max} - E_{min}).$$

where $T^{(m)}$ is the cycle length determined by the sequence of $\{P_i^{(m)}\}_{i=1,2,\ldots,n}$.

Note that

$$T^{(m)} = \frac{E_{max} - E_{min}}{P_{max}^{(m)}} + \frac{E_{max} - E_{min}}{U - P_{max}^{(m)}}. \tag{15}$$

and $P_{max}^{(m)} = P_m^{(m)}$ are the same for all $m = 1,2,\ldots,n$, then $T^{(m)}$ are the same for all $m = 1,2,\ldots,n$.

Note that

$$\frac{T^{(1)}}{U}\sum_{k=1}^{n} P_k^{(1)} + \sum_{k=1}^{n-1} t_{k,k+1} + t_{n,0} \geq \frac{T^{(m)}}{U}\sum_{k=m}^{n} P_k^{(m)} + \sum_{k=m}^{n-1} t_{k,k+1} + t_{n,0}.$$

then we can conclude that if condition(I) is not satisfied when $m = 1$, then it cannot be satisfied when $m > 1$, $i.e.$ if $E_1^{(1)} > E_{max}$, then $E_m^{(m)} > E_{max}$.

With the lemma and remark above, if existing sensors which solved $E_i > E_{max}$, we could adjust the energy consumption rate of the first node on the tsp path to $\frac{U-\sqrt{U^2-4UP_{max}}}{2}$(by having the sensor node discharge at this rate) , all the other nodes except the first one will satisfy $E_i \leq E_{max}$. But it may occur that the $E_1 \geq E_{max}$, we have:

$$E_1^{(1)} = (T^{(1)} - \frac{T^{(1)}}{U}\sum_{k=1}^{n} P_k^{(1)} - \sum_{k=1}^{n-1} t_{k,k+1} - t_{n,0})P_1^{(1)} + E_{min}. \tag{16}$$

if

$$\triangle E_1 = E_1^{(1)} - E_{max} > 0. \tag{17}$$

We give the first node an additional battery with the capacity of $\triangle E_1$, which is very small in practical applications. If equation (17) doesn't satisfy, we only need to adjust the energy consumption rate of the first node on Tsp. In conclusion, we utilize the following Algorithm 2 to construct renewable cycles.

Table 1. Construction of Renewable cycles

Algorithm 2. Construction of Renewable cycles

1: Reindex each sensor node according to Tsp as in Algorithm 1.
2: Test condition(I) and (II) in Lemma 2 for each node.
3: **if** condition (I) and (II) satisfied **then**
4: Execute Algorithm 1
5: **else**
6: Adjust P_1 to $P_1^{(1)}$ as in Lemma 3.
7: Calculate $T = T^{(m)}$ by solving (25).
8: **if** $\triangle E_1 > 0$ **then**
9: Add additional battery capacity of $\triangle E_1$ to node 1.
10: Execute Algorithm 1

4. Construction of Initialization Cycles

Note that all sensor nodes have an energy level of E_{max} when they are first started, our goal is to have each sensor nodes possessing an initial energy level of E_i solved in section 3.3 in the following renewable cycles. In this section, we'll show how to construct initialization cycles.

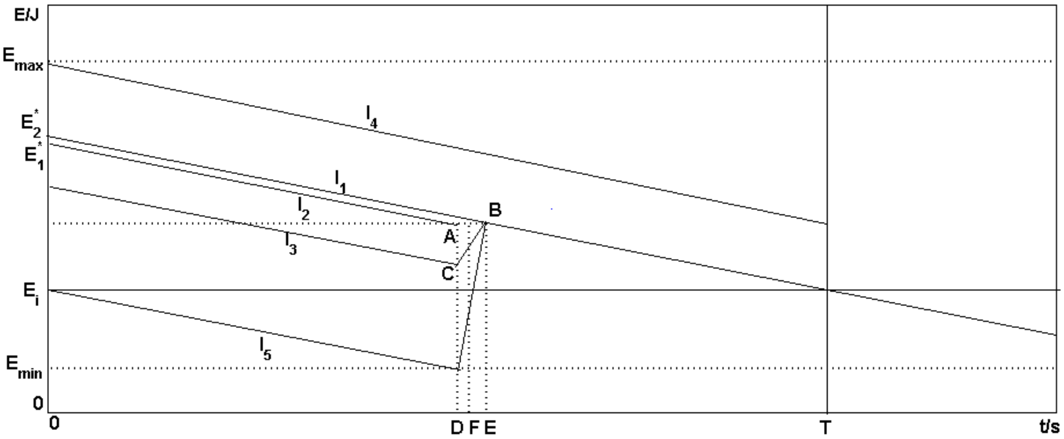

Fig. 4. An example of initialization cycles.

As shown in **Fig. 4**, we depict three situations which might occur during initialization cycles. l_5 shows a normal renewable cycle of node i which we want to achieve after the initialization. In our initialization cycles, the energy dynamics is consistent with renewable cycles and the cycle time is the same as T^*solved in renewable cycles. $t = t_2^{(i)}$ is the WCV's arrival time point at node i shown as point D. During time $[t_2^{(i)}, t_2^{(i)} + t_i]$, node i receives energy from WCV at a rate of U_i. l_1 shows that when the initial energy of node i in an initialization cycle which is denoted as $E_o(i)$ is E_2^*, the energy level will fall to exactly E_i at the end of this cycle. Accordingly, when the initial energy level is above E_2^* and below E_{max}, WCV just waits (close its energy transfer module) at node i for time t_i without transferring energy. Let $E_m(i)$ denote the energy level of node i when WCV finishes charging in a renewable cycle and $E_m(i) = E_{min} + (U_{Full} - P_i) \cdot \frac{P_i T}{U_{Full}}$, which is also the maximum energy level a node i can obtain in a renewable cycle. As in section 3.2, we solve $A(\frac{E_i - E_{min}}{P_i}, E_m(i)), B(\frac{E_i - E_{min}}{P_i} + \frac{P_i T}{U_{Full}}, E_m(i))$ and have:

$$E_2^* = E_i + P_i T. \tag{18}$$

$$E_1^* = E_i + (U_{Full} - P_i) t_i. \tag{19}$$

Secondly, when $E_o(i)$ is between E_1^* and E_2^*, WCV needs to wait for some time $WT(i)$ after arriving at node i at $t_i^{(2)}$ and then charges the node at the rate of P_i by keeping a certain distance from node i. The energy decreasing line with a slope of $-P_i$ between l_1 and l_2 will intersect $E = E_m(i)$ at a point, suppose P, then the difference between WCV arrival time(D) and the horizontal axis of P(e.g. point F) is $WT(i)$ for WCV to wait at node i. Assume $E_1^* \geq E_o(i) \leq E_2^*$, we get:

$$WT(i) = \frac{E_o(i) - E_{min} - (U_{Full} - P_i)t_i}{P_i} - \frac{E_i - E_{min}}{P_i} \\ = \frac{E_o(i) - E_i - (U_{Full} - P_i)t_i}{P_i}. \tag{20}$$

Certainly, to fit the energy dynamic at node i, then the charging time $CT(i)$ is:

$$CT(i) = t_i - WT(i). \tag{21}$$

In the third case when $E_i \leq E_o(i) < E_1^*$ (shown as l_3), WCV charges the node as soon as it arrives at the rate of U_i for node i to receive energy. Note that $U_i - P_i$ is the new slope during t_i, we solve this U_i by calculating $B(\frac{E_i - E_{min}}{P_i} + \frac{P_i T}{U_{Full}}, (U_{Full} - P_i) \cdot \frac{P_i T}{U_{Full}} + E_{min})$, $C(\frac{E_i - E_{min}}{P_i}, E_o(i) + E_{min} - E_i)$, then $U_i - P_i = K_{BC}$ (the slope of BC). After simplifying we get: $U_i = U_{Full} \cdot (1 - \frac{E_o(i) - E_i}{P_i T})$, with the definition of $\mu(i)$ in section 2.1, we have:

$$\mu(i) = 1 - \frac{E_o(i) - E_i}{P_i T}. \tag{22}$$

Note that the new $U_i < U_{Full}$, to achieve equation (22), WCV must charge sensor node within a distance and we could get this distance by solving $D(i)$ in equation (3).

Procedure 1. Let $position(i)$ denote the coordinate of node i in the plane where WSN lies. The arrival position of WCV at node i is updated by letting $position(i).x = position(i).x + D(i)$, $position(i).y = position(i).y$.

By choosing a point on the circumference of the circle which is centered at sensor node i with a radius of $D(i)$, we get the WCV's new arrival position at node i. Again, to accord with the energy dynamics in renewable cycles, we need to adjust the speed of WCV from node i to its next destination, e.g. node j, according to the new arrival position, i.e. let $\frac{d_{i,j}}{V} = \frac{d_(i,j)^*}{V_N(i)}$, where $d_{i,j}$ is the distance is the distance between node i and j, $d_{i,j}^*$ is the new distance between the new arrival position at node i and j, V is the constant speed of WCV in renewable cycles and $V_N(i)$ is the new speed for WCV to move from node i to j. As the initialization cycles proceed, more and more nodes enter into their renewable cycles, which can be observed in our later simulation results. The total initialization cycles end when all nodes enter their renewable cycles. Denote R_{IC} as the total rounds of initialization cycles, we have

$$R_{IC} = \lfloor max\{\frac{E_m ax - E_i}{P_i T}\}\rfloor. \tag{23}$$

which is easy to explain that the last node to enter into its renewable cycles determines how many rounds it needs to take for completing the whole initialization cycles.

5. Numerical Results

In this section, we present some simulation results to show how our construction algorithms are implemented to solve the optimal objective for wireless energy transfer in WSNs.

5.1 Simulation Settings

We consider 100 sensor nodes are randomly deployed over a $1000 \times 1000m^2$ square area. The data flow rate, i.e., f_{ij}, f_{iB} for each sensor node are generated satisfying equation (6) within $1 \sim 10$ kb/s. The energy consumption rate P_i can be obtained by solving equation (7). The power consumption coefficients are $\varepsilon_1 = 50nJ/b, \varepsilon_2 = 0.0013pJ/(b \cdot m^4)$, $\sigma = 50nJ/b$, $\alpha = 4$ [18]. The base station in our simulation environment is located at (570,590)(in m) and the service station for WCV is at (50,50)(in m). The constant traveling speed of WCV in renewable cycles is set as 5 m/s. As for the battery used for providing energy for sensor nodes, we choose a regular NiMH battery and its nominal cell voltage and volume of electricity is 1.2V/2.5Ah. To make a comparison with [9], we have $E_{max} = 1.2V \times 10.8KJ \times 3600sec = 10.8KJ$ [19], $E_{min} = 0.05 \times E_{max} = 540J$. We assume the wireless energy transfer rate $U_{Full} = 30$ W which is within the feasible range in [6, 22].

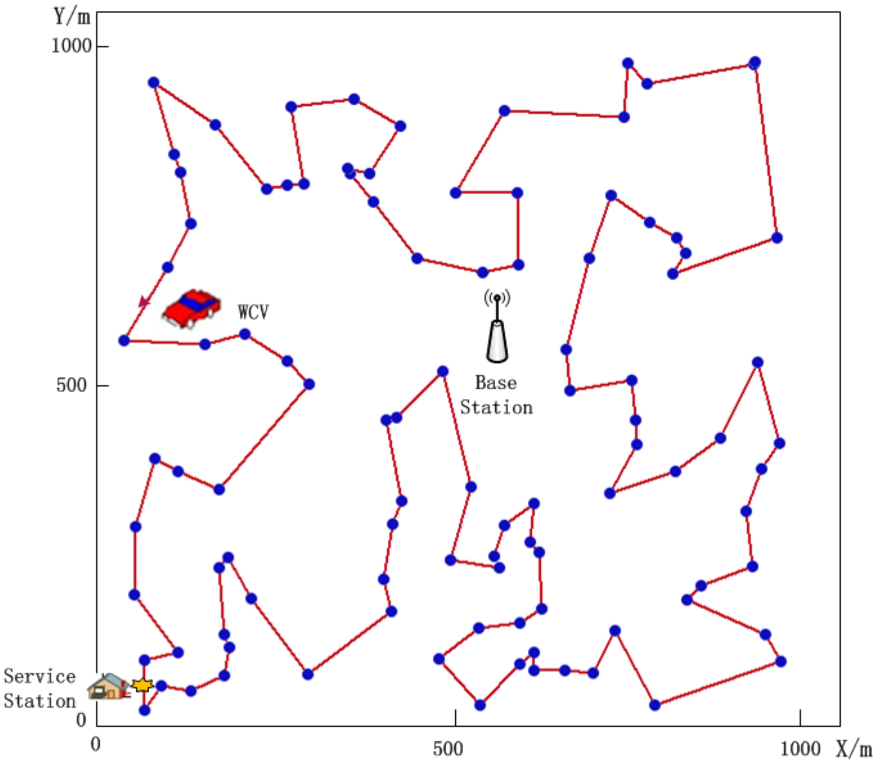

Fig. 5. The Tsp path found by Concorde in a 100-node WSN.

5.2 Results and Analysis

We find the shortest Hamiltonian cycle (Tsp path) with Concorde solver [20] as shown in **Fig. 5**. Note that the traveling direction of WCV–whether to travel along the clockwise direction or counter clockwise–has no influence in our solution to the objective value $\frac{T_{vac}}{T}$, because they all achieve the same T_p. In our simulation we let the WCV follow the counter clockwise direction and get total travel length $D_{Tsp} = 8020.88$ m, $T_p = 1604.18$ s. As presented in Algorithm 2, we first solve E_i for each node and for our generated data, there is no need to adjust the energy consumption rate of node 1. We find that a higher energy consumption rate P_i is often accompanied with a higher E_i, which indicates that the traveling order to some extent plays a minor role in determining E_i. This property is also helpful in a practical WSN, since sensor nodes closer to sink node take over a heavier traffic load and need more initial energy capacity to sustain the cycle compared to other nodes, The overall cycle time $T = 61053$s (i.e. T^*), the optimal objective value $\frac{T_{vac}}{T} = 62.51\%$.

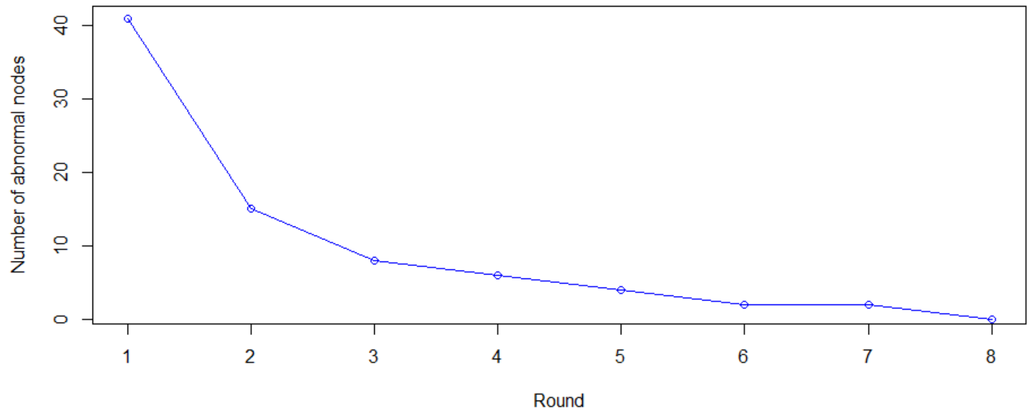

Fig. 6. Number of abnormal nodes in initialization cycles.

In experiment, it takes 8 rounds for every node to enter into their renewable cycles. We call nodes that haven't come to renewable cycles "abnormal nodes", and **Fig. 6** shows the number of abnormal nodes at the end of each round through initialization cycles. Note that when the second round ends, 85% nodes have obtained an initial energy level of E_i and start their renewable energy cycles, which is a high-efficient transition for WSN. Due to space limitation, detailed simulation results on initialization cycles are provided in [22]. We choose three nodes and give the WCV's performance at them under our settings in **Table 2**, in which node 7 enters into renewable cycle with 1 round and 2 rounds for node 41, 8 rounds for node 52.

Table 2. WCV performance at node 7,41,52 in initialization cycles

Node index	travel order	Round	$V_N(i)$ m/s	CT(i) (s)	U_i (W)	R_i (m)	$WT(i)$ (s)
7	30	1	5.011	223.86	6.185	2.689	0
41	60	1	5.066	0	0	0	81.404
		2	5	0	0	0	81.404
		3	5	0	0	0	81.404
		4	4.95	81.404	19.24	1.749	0
52	10	1	5	0	0	0	42.737
		2	5.066	0	0	0	42.737
		3	5	0	0	0	42.737
		4	5	0	0	0	42.737
		5	5	0	0	0	42.737
		6	5	0	0	0	42.737
		7	5	0	0	0	42.737
		8	4.956	42.737	19.73	1.704	0

5.3 Extending Discussions

Naturally, when the scale of wireless sensor network is extended with thousands of nodes deployed, one mobile charger is not sufficient to serve for the overall WSN. Therefore, several WCVs are needed to accomplish charging tasks. As mentioned in section 2.1, by partitioning the field where WSN is deployed, our model can be extended in a more complicated scenario. Since sensor nodes are usually uniformly scattered in an area, we can leave out the sensor nodes' density problem here. The minimum number of WCVs needed should satisfy the need of charging tasks and achieve the minimum cost of mobile cars in the meanwhile. Given a partition scheme and the initial position of WCV in each subarea (a WCV serves in only one subarea), we can work out the renewable cycles including T, T_p, T_c and the energy needed for charging and traveling in one cycle in a subarea can be calculated as well. To determine the minimum number of WCVs, we implement a heuristic algorithm: First set the expected objective threshold. For each partition (from 1 to n ⊆ N), checking if the condition of WCV meets the energy constraints and objective value can be obtained. The first partition number meeting the check is the minimum number of WCVs needed.

6. Conclusion

To address energy limitation problem in a practical large-scale wireless sensor network, taking advantage of the breakthrough in wireless energy transfer technology, we proposed two feasible and provable algorithms for the optimal charging scheduling in renewable energy cycles. A wireless charging vehicle (WCV) is employed to charge each sensor node wirelessly along the Tsp path in this problem. To enable our algorithm be applied in a large-scale WSN, we studied the optimization problem based on existing and practical WSNs, with the objective of maximizing the ratio of the WCV’s vacation time at service station over the cycle time. We designed two algorithms for constructing initialization cycles and renewable cycles respectively with solid theoretical analysis, which achieves the optimal objective. Our complete numerical results showed the detailed charging behavior of WCV both in initialization cycles and renewable cycles in our optimal solution and demonstrated the effectiveness of our algorithms.

References

[1] A. Dunkels, F. Ö sterlind, and Z. He, “An adaptive communication architecture for wireless sensor networks,” in *Proc. of the 5th international conference on Embedded networked sensor systems, ACM*, 2007. Article (CrossRef Link)

[2] W. Wang, V. Srinivasan, and K.-C. Chua, “Using mobile relays to prolong the lifetime of wireless sensor networks,” in *Proc. of ACM MobiCom*, 2005. Article (CrossRef Link)

[3] A. Kansal, J. Hsu, S. Zahedi, and M. B. Srivastava, “Power management in energy harvesting sensor networks,” *ACM Transactions on Embedded Computing Systems (TECS)*, vol. 6, no. 4, p. 32, 2007. Article (CrossRef Link)

[4] X. Jiang, J. Polastre, and D. Culler, “Perpetual environmentally powered sensor networks,” in *Proc. of IEEE IPSN*, 2005. Article (CrossRef Link)

[5] B. Tong, G. Wang, W. Zhang, and C. Wang, “Node reclamation and replacement for long-lived sensor networks,” *IEEE Transactions on Parallel and Distributed Systems*, vol. 22, no. 9, pp. 1550–1563, 2011. Article (CrossRef Link)

[6] A. Kurs, A. Karalis, R. Moffatt, J. D. Joannopoulos, P. Fisher, and M. Soljacic, "Wireless power transfer via strongly coupled magnetic resonances," *science*, vol. 317, no. 5834, pp. 83–86, 2007. Article (CrossRef Link)

[7] "Wireless resonant energy link (wrel) demo," http://software.intel.com/en-us/videos/wireless-resonant-energy-linkwrel-demo/.

[8] S. Guo, C. Wang, and Y. Yang, "Mobile data gathering with wireless energy replenishment in rechargeable sensor networks," in *Proc. of IEEE INFOCOM*, 2013. Article (CrossRef Link)

[9] Y. Shi, L. Xie, Y. T. Hou, and H. D. Sherali, "On renewable sensor networks with wireless energy transfer," in *Proc. of IEEE INFOCOM*, 2011. Article (CrossRef Link)

[10] L. Xie, Y. Shi, Y. T. Hou, W. Lou, H. D. Sherali, and S. F. Midkiff, "On renewable sensor networks with wireless energy transfer: The multi-node case," in IEEE SECON, 2012. Article (CrossRef Link)

[11] Z. Li, Y. Peng, W. Zhang, and D. Qiao, "J-roc: A joint routing and charging scheme to prolong sensor network lifetime," in *Proc. of IEEE International Conference on Network Protocols (ICNP)*, 2011. Article (CrossRef Link)

[12] S. Zhang, J. Wu, and S. Lu, "Collaborative mobile charging for sensor networks," in *Proc. of IEEE MASS*, 2012. Article (CrossRef Link)

[13] C. Wang, J. Li, F. Ye, and Y. Yang, "Multi-vehicle coordination for wireless energy replenishment in sensor networks," in *Proc. of IEEE International Symposium on Parallel & Distributed Processing (IPDPS)*, 2013. Article (CrossRef Link)

[14] W. Xu, W. Liang, X. Ren, and X. Lin, "On-demand energy replenishment for sensor networks via wireless energy transfer," in *Proc. of PIMRC, IEEE*, 2014. Article (CrossRef Link)

[15] C. M. Angelopoulos, S. Nikoletseas, and T. P. Raptis, "Efficient wireless recharging in sensor networks," in *Proc. of IEEE International Conference on Distributed Computing in Sensor Systems (DCOSS)*, 2013. Article (CrossRef Link)

[16] Y. T. Hou, Y. Shi, and H. D. Sherali, "Rate allocation and network lifetime problems for wireless sensor networks," *IEEE/ACM Transactions on Networking (TON)*, vol. 16, no. 2, pp. 321–334, 2008. Article (CrossRef Link)

[17] B.Baranidharan, B.Shanthi, "A Survey on Energy Efficient Protocols for Wireless Sensor Networks," *International Journal of Computer Applications*, vol. 11– No.10, December 2010. Article (CrossRef Link)

[18] W. B. Heinzelman, A. P. Chandrakasan, and H. Balakrishnan, "An application-specific protocol architecture for wireless microsensor networks," *IEEE Transactions on Wireless Communications*, vol. 1, no. 4, pp. 660–670, 2002. Article (CrossRef Link)

[19] D. Linden and T. B. Reddy, "Handbook of batteries," New York, vol. 2nd, 2002.

[20] Concorde home. [Online]. Available: http://www.math.uwaterloo.ca/tsp/concorde/index.html

[21] S. Jae-Hyun, K. Yong-Hyuk, R. Hwang-Bin, C. Si-Ho, and J. Minho, "Optimal sensor deployment for wireless surveillance sensor networks by a hybrid steady-state genetic algorithm," *IEICE transactions on communications*, vol. 91, no. 11, pp. 3534–3543, 2008. Article (CrossRef Link)

[22] Technical report and detailed simulation results. [Online]. Available: http://www.lubingxian.cn/Report_wsn.pdf

Zhenquan Qin received the bachelor degree in security engineering and the Ph.D. degree in communication and informatin system both from University of Science and Technology of China (USTC) in 2002 and 2007, respectively. Now he is an associate professor in the School of Software of Dalian University of Technology (DUT). He is a member of IEEE and China Computer Federation (CCF). His research interests include wireless network, network analysis and network security.

Bingxian Lu was born in 1991. He received a Bachelor degree in software engineering in 2012, and an M.E. in 2014 both from Dalian University of Technology, Dalian, China, where he is going for a Ph.D. degree. He is a student member of ACM and China Computer Federation (CCF). His research interests include wireless network, cognitive radio networks, and game theory.

Ming Zhu received the bachelor's and master's degrees in communication and information system from the School of Software, Dalian University of Technology, Dalian, China, where he is currently pursuing the Ph.D. degree. His research interests include wireless sensor networks and wireless networks communications.

Liang Sun is an Engineer in School of Software at Dalian University of Technology, China. He is studying his PhD degree from the Dalian University of Technology. His research interests are in the area of wireless networking and mobile computing. He is particularly interested in algorithm innovation and implementation for IEEE 802.11 wireless local area networks and cognitive radio networks, system modeling and performance analysis of wireless sensor networks.

Lei Shu (M'07) received Ph.D. degree from National University of Ireland, Galway, Ireland, in 2010. Until March 2012, he was a Specially Assigned Researcher in Department of Multimedia Engineering, Graduate School of Information Science and Technology, Osaka University, Japan. Since October 2012, he joined Guangdong University of Petrochemical Technology, China as a full professor. His research interests include: Wireless Sensor Networks, Multimedia Communication, Middleware, Security, and Fault Diagnosis. He has published over 200 papers in related conferences, journals, and books. His current H-index is 17. He had been awarded the*Globecom 2010* and *ICC 2013 Best Paper Award*. He is serving as *Editor in Chief* for *EAI Endorsed Transactions on Industrial Networks and Intelligent Systems*, and associate editors for a number of famous international journals.